

Tevatron Constraints on Models of the Higgs Boson with Exotic Spin and Parity Using Decays to Bottom-Antibottom Quark Pairs

- T. Aaltonen \dagger^{21} V.M. Abazov \ddagger^{13} B. Abbott \ddagger^{116} B.S. Acharya \ddagger^{80} M. Adams \ddagger^{98} T. Adams \ddagger^{97} J.P. Agnew \ddagger^{94}
 G.D. Alexeev \ddagger^{13} G. Alkhazov \ddagger^{88} A. Alton $\ddagger^{jj,31}$ S. Amerio $\ddagger^{yy,39}$ D. Amidei \dagger^{31} A. Anastassov $\ddagger^{w,15}$ A. Annovi
 \dagger^{17} J. Antos \dagger^{12} G. Apollinari \dagger^{15} J.A. Appel \dagger^{15} T. Arisawa \dagger^{52} A. Artikov \dagger^{13} J. Asaadi \dagger^{47} W. Ashmanskas
 \dagger^{15} A. Askew \ddagger^{97} S. Atkins \ddagger^{106} B. Auerbach \dagger^2 K. Augsten \ddagger^{62} A. Aurisano \dagger^{47} C. Avila \ddagger^{60} F. Azfar \dagger^{38}
 F. Badaud \ddagger^{65} W. Badgett \dagger^{15} T. Bae \dagger^{25} L. Bagby \ddagger^{15} B. Baldin \ddagger^{15} D.V. Bandurin \ddagger^{122} S. Banerjee \ddagger^{80}
 A. Barbaro-Galtieri \dagger^{26} E. Barberis \ddagger^{107} P. Baringer \ddagger^{105} V.E. Barnes \dagger^{43} B.A. Barnett \dagger^{23} P. Barria $\ddagger^{aaa,41}$
 J.F. Bartlett \ddagger^{15} P. Bartos \dagger^{12} U. Bassler \ddagger^{70} M. Bauce $\ddagger^{yy,39}$ V. Bazterra \ddagger^{98} A. Bean \ddagger^{105} F. Bedeschi \dagger^{41}
 M. Begalli \ddagger^{57} S. Behari \dagger^{15} L. Bellantoni \ddagger^{15} G. Bellettini $\ddagger^{zz,41}$ J. Bellinger \dagger^{54} D. Benjamin \dagger^{14} A. Beretvas \dagger^{15}
 S.B. Beri \ddagger^{78} G. Bernardi \ddagger^{69} R. Bernhard \ddagger^{74} I. Bertram \ddagger^{92} M. Besançon \ddagger^{70} R. Beuselinck \ddagger^{93} P.C. Bhat \ddagger^{15}
 S. Bhatia \ddagger^{108} V. Bhatnagar \ddagger^{78} A. Bhatti \dagger^{45} K.R. Bland \dagger^5 G. Blazey \ddagger^{99} S. Blessing \ddagger^{97} K. Bloom \ddagger^{109}
 B. Blumenfeld \dagger^{23} A. Bocci \dagger^{14} A. Bodek \dagger^{44} A. Boehnlein \ddagger^{15} D. Boline \ddagger^{113} E.E. Boos \ddagger^{86} G. Borissov \ddagger^{92}
 D. Bortoletto \dagger^{43} M. Borysova $\ddagger^{uu,91}$ J. Boudreau \dagger^{42} A. Boveia \dagger^{11} A. Brandt \ddagger^{119} O. Brandt \ddagger^{75} L. Brigliadori
 $\dagger^{xx,6}$ R. Brock \ddagger^{32} C. Bromberg \dagger^{32} A. Bross \ddagger^{15} D. Brown \ddagger^{69} E. Brucken \dagger^{21} X.B. Bu \ddagger^{15} J. Budagov \dagger^{13}
 H.S. Budd \dagger^{44} M. Buehler \ddagger^{15} V. Buescher \ddagger^{76} V. Bunichev \ddagger^{86} S. Burdin $\ddagger^{kk,92}$ K. Burkett \dagger^{15} G. Busetto $\ddagger^{yy,39}$
 P. Bussey \dagger^{19} C.P. Buszello \ddagger^{90} P. Butti $\ddagger^{zz,41}$ A. Buzatu \dagger^{19} A. Calamba \dagger^{10} E. Camacho-Pérez \ddagger^{83} S. Camarda
 \dagger^{4} M. Campanelli \dagger^{28} F. Canelli $\dagger^{dd,11}$ B. Carls \dagger^{22} D. Carlsmith \dagger^{54} R. Carosi \dagger^{41} S. Carrillo $\dagger^{ll,16}$ B. Casal $\dagger^{j,9}$
 M. Casarsa \dagger^{48} B.C.K. Casey \ddagger^{15} H. Castilla-Valdez \ddagger^{83} A. Castro $\dagger^{xx,6}$ P. Catastini \dagger^{20} S. Caugron \ddagger^{32} D. Cauz
 $\dagger^{ffffggg,48}$ V. Cavaliere \dagger^{22} A. Cerri $\dagger^{ee,26}$ L. Cerrito $\dagger^{rr,28}$ S. Chakrabarti \ddagger^{113} K.M. Chan \ddagger^{103} A. Chandra \ddagger^{121}
 E. Chapon \ddagger^{70} G. Chen \ddagger^{105} Y.C. Chen \dagger^1 M. Chertok \dagger^7 G. Chiarelli \dagger^{41} G. Chlachidze \dagger^{15} K. Cho \dagger^{25}
 S.W. Cho \ddagger^{82} S. Choi \ddagger^{82} D. Chokheli \dagger^{13} B. Choudhary \ddagger^{79} S. Cihangir \ddagger^{15} D. Claes \ddagger^{109} A. Clark \dagger^{18} C. Clarke
 \dagger^{53} J. Clutter \ddagger^{105} M.E. Convery \dagger^{15} J. Conway \dagger^{7} M. Cooke $\ddagger^{tt,15}$ W.E. Cooper \ddagger^{15} M. Corbo $\dagger^{zz,15}$ M. Corcoran
 \ddagger^{121} M. Cordelli \dagger^{17} F. Couderc \ddagger^{70} M.-C. Cousinou \ddagger^{67} C.A. Cox \dagger^7 D.J. Cox \dagger^7 M. Cremonesi \dagger^{41} D. Cruz \dagger^{47}
 J. Cuevas $\dagger^{yy,9}$ R. Culbertson \dagger^{15} D. Cutts \ddagger^{118} A. Das \ddagger^{120} N. d'Ascenzo $\dagger^{vv,15}$ M. Datta $\dagger^{gg,15}$ G. Davies \ddagger^{93}
 P. de Barbaro \dagger^{44} S.J. de Jong $\ddagger^{84,85}$ E. De La Cruz-Burelo \ddagger^{83} F. Déliot \ddagger^{70} R. Demina \ddagger^{44} L. Demortier \dagger^{45}
 M. Deninno \dagger^{6} D. Denisov \ddagger^{15} S.P. Denisov \ddagger^{87} M. D'Errico $\ddagger^{yy,39}$ S. Desai \ddagger^{15} C. Deterre $\dagger^{ll,94}$ K. DeVaughan
 \dagger^{109} F. Devoto \dagger^{21} A. Di Canto $\dagger^{zz,41}$ B. Di Ruza $\dagger^{pp,15}$ H.T. Diehl \ddagger^{15} M. Diesburg \ddagger^{15} P.F. Ding \ddagger^{94}
 J.R. Dittmann \dagger^{5} A. Dominguez \ddagger^{109} S. Donati $\ddagger^{zz,41}$ M. D'Onofrio \dagger^{27} M. Dorigo $\dagger^{hhh,48}$ A. Driutti $\dagger^{ffffggg,48}$
 A. Dubey \ddagger^{79} L.V. Dudko \ddagger^{86} A. Duperrin \ddagger^{67} S. Dutt \ddagger^{78} M. Eads \ddagger^{99} K. Ebina \dagger^{52} R. Edgar \dagger^{31} D. Edmunds
 \ddagger^{32} A. Elagin \dagger^{47} J. Ellison \ddagger^{96} V.D. Elvira \ddagger^{15} Y. Enari \ddagger^{69} R. Erbacher \dagger^7 S. Errede \dagger^{22} B. Esham \dagger^{22} H. Evans
 \ddagger^{101} V.N. Evdokimov \ddagger^{87} S. Farrington \dagger^{38} A. Fauré \ddagger^{70} L. Feng \ddagger^{99} T. Ferbel \ddagger^{44} J.P. Fernández Ramos \dagger^{29}
 F. Fiedler \ddagger^{76} R. Field \dagger^{16} F. Filthaut $\ddagger^{84,85}$ W. Fisher \ddagger^{32} H.E. Fisk \ddagger^{15} G. Flanagan $\dagger^{tt,15}$ R. Forrest \dagger^7
 M. Fortner \ddagger^{99} H. Fox \ddagger^{92} M. Franklin \dagger^{20} J.C. Freeman \dagger^{15} H. Frisch \dagger^{11} S. Fuess \ddagger^{15} Y. Funakoshi \dagger^{52}
 C. Galloni $\ddagger^{zz,41}$ P.H. Garbincius \ddagger^{15} A. Garcia-Bellido \ddagger^{44} J.A. García-González \ddagger^{83} A.F. Garfinkel \dagger^{43} P. Garosi
 $\ddagger^{aaa,41}$ V. Gavrilov \ddagger^{33} W. Geng $\ddagger^{67,32}$ C.E. Gerber \ddagger^{98} H. Gerberich \dagger^{22} E. Gerchtein \dagger^{15} Y. Gershtein \ddagger^{110}
 S. Giagu \dagger^{46} V. Giakoumopoulou \dagger^3 K. Gibson \dagger^{42} C.M. Ginsburg \ddagger^{15} G. Ginther $\ddagger^{15,44}$ N. Giokaris \dagger^3
 P. Giromini \dagger^{17} V. Glagolev \dagger^{13} D. Glenzinski \dagger^{15} O. Gogota \ddagger^{91} M. Gold \dagger^{34} D. Goldin \dagger^{47} A. Golossanov \dagger^{15}
 G. Golovanov \ddagger^{13} G. Gomez \dagger^{9} G. Gomez-Ceballos \dagger^{30} M. Goncharov \dagger^{30} O. González López \dagger^{29} I. Gorelov \dagger^{34}
 A.T. Goshaw \dagger^{14} K. Goulianatos \dagger^{45} E. Gramellini \dagger^6 P.D. Grannis \ddagger^{113} S. Greder \ddagger^{71} H. Greenlee \ddagger^{15} G. Grenier
 \ddagger^{72} Ph. Gris \ddagger^{65} J.-F. Grivaz \ddagger^{68} A. Grohsjean $\dagger^{ll,70}$ C. Grossi-Pilcher \dagger^{11} R.C. Group $\dagger^{51,15}$ S. Grünenwald \ddagger^{15}
 M.W. Grünewald \ddagger^{81} T. Guillemin \ddagger^{68} J. Guimaraes da Costa \dagger^{20} G. Gutierrez \ddagger^{15} P. Gutierrez \ddagger^{116} S.R. Hahn
 \dagger^{15} J. Haley \ddagger^{117} J.Y. Han \dagger^{44} L. Han \ddagger^{59} F. Happacher \dagger^{17} K. Hara \dagger^{49} K. Harder \ddagger^{94} M. Hare \dagger^{50} A. Harel \ddagger^{44}
 R.F. Harr \dagger^{53} T. Harrington-Taber $\dagger^{mm,15}$ K. Hatakeyama \dagger^5 J.M. Hauptman \ddagger^{104} C. Hays \dagger^{38} J. Hays \ddagger^{93}
 T. Head \ddagger^{94} T. Hebbeker \ddagger^{73} D. Hedin \ddagger^{99} H. Hegab \ddagger^{117} J. Heinrich \dagger^{40} A.P. Heinson \ddagger^{96} U. Heintz \ddagger^{118}
 C. Hensel \ddagger^{56} I. Heredia-De La Cruz $\ddagger^{mm,83}$ M. Herndon \dagger^{54} K. Herner \ddagger^{15} G. Hesketh $\ddagger^{oo,94}$ M.D. Hildreth \ddagger^{103}

R. Hirosky †, 122 T. Hoang †, 97 J.D. Hobbs †, 113 A. Hocker †, 15 B. Hoeneisen †, 64 J. Hogan †, 121 M. Hohlfeld †, 76
J.L. Holzbauer †, 108 Z. Hong †, 47 W. Hopkins †^f, 15 S. Hou †, 1 I. Howley †, 119 Z. Hubacek †, 62, 70 R.E. Hughes †, 35
U. Husemann †, 55 M. Hussein †^{bb}, 32 J. Huston †, 32 V. Hynek †, 62 I. Iashvili †, 112 Y. Ilchenko †, 120 R. Illingworth †, 15
G. Introzzi †^{ccccdd}, 41 M. Iori †^{eee}, 46 A.S. Ito †, 15 A. Ivanov †^o, 7 S. Jabeen †^{vv}, 15 M. Jaffré †, 68 E. James †, 15 D. Jang
†, 10 A. Jayasinghe †, 116 B. Jayatilaka †, 15 E.J. Jeon †, 25 M.S. Jeong †, 82 R. Jesik †, 93 P. Jiang †, 59 S. Jindariani †, 15
K. Johns †, 95 E. Johnson †, 32 M. Johnson †, 15 A. Jonckheere †, 15 M. Jones †, 43 P. Jonsson †, 93 K.K. Joo †, 25 J. Joshi
†, 96 S.Y. Jun †, 10 A.W. Jung †, 15 T.R. Junk †, 15 A. Juste †, 89 E. Kajfasz †, 67 M. Kambeitz †, 24 T. Kamon †, 25, 47
P.E. Karchin †, 53 D. Karmanov †, 86 A. Kasmi †, 5 Y. Kato †ⁿ, 37 I. Katsanos †, 109 M. Kaur †, 78 R. Kehoe †, 120
S. Kermiche †, 67 W. Ketchum †^{hh}, 11 J. Keung †, 40 N. Khalatyan †, 15 A. Khanov †, 117 A. Kharchilava †, 112
Y.N. Kharzhev †, 13 B. Kilminster †^{dd}, 15 D.H. Kim †, 25 H.S. Kim †, 25 J.E. Kim †, 25 M.J. Kim †, 17 S.H. Kim †, 49
S.B. Kim †, 25 Y.J. Kim †, 25 Y.K. Kim †, 11 N. Kimura †, 52 M. Kirby †, 15 I. Kiselevich †, 33 K. Knoepfel †, 15
J.M. Kohli †, 78 K. Kondo †, 52, * D.J. Kong †, 25 J. Konigsberg †, 16 A.V. Kotwal †, 14 A.V. Kozelov †, 87 J. Kraus †, 108
M. Kreps †, 24 J. Kroll †, 40 M. Kruse †, 14 T. Kuhr †, 24 A. Kumar †, 112 A. Kupco †, 63 M. Kurata †, 49 T. Kurča †, 72
V.A. Kuzmin †, 86 A.T. Laasanen †, 43 S. Lammel †, 15 S. Lammers †, 101 M. Lancaster †, 28 K. Lannon †^x, 35 G. Latino
†^{aaa}, 41 P. Lebrun †, 72 H.S. Lee †, 82 H.S. Lee †, 25 J.S. Lee †, 25 S.W. Lee †, 104 W.M. Lee †, 15 X. Lei †, 95 J. Lellouch
†, 69 S. Leo †, 22 S. Leone †, 41 J.D. Lewis †, 15 D. Li †, 69 H. Li †, 122 L. Li †, 96 Q.Z. Li †, 15 J.K. Lim †, 82 A. Limosani
†^s, 14 D. Lincoln †, 15 J. Linnemann †, 32 V.V. Lipaev †, 87 E. Lipeles †, 40 R. Lipton †, 15 A. Lister †^a, 18 H. Liu †, 51
H. Liu †, 120 Q. Liu †, 43 T. Liu †, 15 Y. Liu †, 59 A. Lobodenko †, 88 S. Lockwitz †, 55 A. Loginov †, 55 M. Lokajicek †, 63
R. Lopes de Sa †, 15 D. Lucchesi †^{yy}, 39 A. Lucà †, 17 J. Lueck †, 24 P. Lujan †, 26 P. Lukens †, 15 R. Luna-Garcia
†^{pp}, 83 G. Lungu †, 45 A.L. Lyon †, 15 J. Lys †, 26 R. Lysak †^d, 12 A.K.A. Maciel †, 56 R. Madar †, 74 R. Madrak
†, 15 P. Maestro †^{aaa}, 41 R. Magaña-Villalba †, 83 S. Malik †, 45 S. Malik †, 109 V.L. Malyshev †, 13 G. Manca
†^b, 27 A. Manousakis-Katsikakis †, 3 J. Mansour †, 75 L. Marchese †ⁱⁱ, 6 F. Margaroli †, 46 P. Marino †^{bbb}, 41
J. Martínez-Ortega †, 83 K. Matera †, 22 M.E. Mattson †, 53 A. Mazzacane †, 15 P. Mazzanti †, 6 R. McCarthy †, 113
C.L. McGivern †, 94 R. McNulty †, 27 A. Mehta †, 27 P. Mehtala †, 21 M.M. Meijer †, 84, 85 A. Melnitchouk †, 15
D. Menezes †, 99 P.G. Mercadante †, 58 M. Merkin †, 86 C. Mesropian †, 45 A. Meyer †, 73 J. Meyer †^{rr}, 75 T. Miao †, 15
F. Miconi †, 71 D. Mietlicki †, 31 A. Mitra †, 1 H. Miyake †, 49 S. Moed †, 15 N. Moggi †, 6 N.K. Mondal †, 80 C.S. Moon
†^z, 15 R. Moore †^{eff}, 15 M.J. Morello †^{bbb}, 41 A. Mukherjee †, 15 M. Mulhearn †, 122 Th. Muller †, 24 P. Murat †, 15
M. Mussini †^{xx}, 6 J. Nachtman †^m, 15 Y. Nagai †, 49 J. Naganoma †, 52 E. Nagy †, 67 I. Nakano †, 36 A. Napier †, 50
M. Narain †, 118 R. Nayyar †, 95 H.A. Neal †, 31 J.P. Negret †, 60 J. Nett †, 47 C. Neu †, 51 P. Neustroev †, 88 H.T. Nguyen
†, 122 T. Nigmanov †, 42 L. Nodulman †, 2 S.Y. Noh †, 25 O. Norniella †, 22 T. Nunnemann †, 77 L. Oakes †, 38 S.H. Oh
†, 14 Y.D. Oh †, 25 I. Oksuzian †, 51 T. Okusawa †, 37 R. Orava †, 21 J. Orduna †, 121 L. Ortolan †, 4 N. Osman †, 67
J. Osta †, 103 C. Pagliarone †, 48 A. Pal †, 119 E. Palencia †^e, 9 P. Palni †, 34 V. Papadimitriou †, 15 N. Parashar †, 102
V. Parihar †, 118 S.K. Park †, 82 W. Parker †, 54 R. Partridge †ⁿⁿ, 118 N. Parua †, 101 A. Patwa †^{ss}, 114 G. Pauletta
†^{ffffggg}, 48 M. Paulini †, 10 C. Paus †, 30 B. Penning †, 15 M. Perfilov †, 86 Y. Peters †, 94 K. Petridis †, 94 G. Petrillo †, 44
P. Pétroff †, 68 T.J. Phillips †, 14 G. Piacentino †^q, 15 E. Pianori †, 40 J. Pilot †, 7 K. Pitts †, 22 C. Plager †, 8 M.-A. Pleier
†, 114 V.M. Podstavkov †, 15 L. Pondrom †, 54 A.V. Popov †, 87 S. Poprocki †^f, 15 K. Potamianos †, 26 A. Pranko †, 26
M. Prewitt †, 121 D. Price †, 94 N. Prokopenko †, 87 F. Prokoshin †^{aa}, 13 F. Ptohos †^g, 17 G. Punzi †^{zz}, 41 J. Qian †, 31
A. Quadt †, 75 B. Quinn †, 108 P.N. Ratoff †, 92 I. Razumov †, 87 I. Redondo Fernández †, 29 P. Renton †, 38 M. Rescigno
†, 46 F. Rimondi †, 6, * I. Ripp-Baudot †, 71 L. Ristori †, 41, 15 F. Rizatdinova †, 117 A. Robson †, 19 T. Rodriguez †, 40
S. Rolli †^h, 50 M. Rominsky †, 15 M. Ronzani †^{zz}, 41 R. Roser †, 15 J.L. Rosner †, 11 A. Ross †, 92 C. Royon †, 70
P. Rubinov †, 15 R. Ruchti †, 103 F. Ruffini †^{aaa}, 41 A. Ruiz †, 9 J. Russ †, 10 V. Rusu †, 15 G. Sajot †, 66 W.K. Sakamoto
†, 44 Y. Sakurai †, 52 A. Sánchez-Hernández †, 83 M.P. Sanders †, 77 L. Santi †^{ffffggg}, 48 A.S. Santos †^{qq}, 56 K. Sato †, 49
G. Savage †, 15 V. Saveliev †^v, 15 M. Savitskyi †, 91 A. Savoy-Navarro †^z, 15 L. Sawyer †, 106 T. Scanlon †, 93
R.D. Schamberger †, 113 Y. Scheglov †, 88 H. Schellman †, 100 P. Schlabach †, 15 E.E. Schmidt †, 15 C. Schwanenberger
†, 94 T. Schwarz †, 31 R. Schwienhorst †, 32 L. Scodellaro †, 9 F. Scuri †, 41 S. Seidel †, 34 Y. Seiya †, 37 J. Sekaric †, 105
A. Semenov †, 13 H. Severini †, 116 F. Sforza †^{zz}, 41 E. Shabalina †, 75 S.Z. Shalhout †, 7 V. Shary †, 70 S. Shaw †, 94
A.A. Shchukin †, 87 T. Shears †, 27 P.F. Shepard †, 42 M. Shimojima †^u, 49 M. Shochet †, 11 I. Shreyber-Tecker †, 33
V. Simak †, 62 A. Simonenko †, 13 P. Skubic †, 116 P. Slattery †, 44 K. Sliwa †, 50 D. Smirnov †, 103 J.R. Smith †, 7
F.D. Snider †, 15 G.R. Snow †, 109 J. Snow †, 115 S. Snyder †, 114 S. Söldner-Rembold †, 94 H. Song †, 42 L. Sonnenschein
†, 73 V. Sorin †, 4 K. Soustruznik †, 61 R. St. Denis †, 19, * M. Stancari †, 15 J. Stark †, 66 D. Stentz †^w, 15 D.A. Stoyanova
†, 87 M. Strauss †, 116 J. Strogas †, 34 Y. Sudo †, 49 A. Sukhanov †, 15 I. Suslov †, 13 L. Suter †, 94 P. Svoisky †, 116

K. Takemasa \dagger^{49} Y. Takeuchi \dagger^{49} J. Tang \dagger^{11} M. Tecchio \dagger^{31} P.K. Teng \dagger^1 J. Thom $\dagger f^{15}$ E. Thomson \dagger^{40}
V. Thukral \dagger^{47} M. Titov \ddagger^{70} D. Toback \dagger^{47} S. Tokar \dagger^{12} V.V. Tokmenin \ddagger^{13} K. Tollefson \dagger^{32} T. Tomura \dagger^{49}
D. Tonelli $\dagger e^{15}$ S. Torre \dagger^{17} D. Torretta \dagger^{15} P. Totaro \dagger^{39} M. Trovato $\dagger bbb^{41}$ Y.-T. Tsai \ddagger^{44} D. Tsybychev \dagger^{113}
B. Tuchming \ddagger^{70} C. Tully \ddagger^{111} F. Ukegawa \dagger^{49} S. Uozumi \dagger^{25} L. Uvarov \ddagger^{88} S. Uvarov \ddagger^{88} S. Uzunyan \ddagger^{99}
R. Van Kooten \ddagger^{101} W.M. van Leeuwen \ddagger^{84} N. Varelas \ddagger^{98} E.W. Varnes \ddagger^{95} I.A. Vasilyev \ddagger^{87} F. Vázquez $\dagger l^{16}$
G. Velev \dagger^{15} C. Vellidis \dagger^{15} A.Y. Verkheev \ddagger^{13} C. Vernieri $\dagger bbb^{41}$ L.S. Vertogradov \ddagger^{13} M. Verzocchi \dagger^{15}
M. Vesterinen \ddagger^{94} M. Vidal \dagger^{43} D. Vilanova \ddagger^{70} R. Vilar \dagger^9 J. Vizán $\dagger cc^{9}$ M. Vogel \dagger^{34} P. Vokac \ddagger^{62} G. Volpi \dagger^{17}
P. Wagner \dagger^{40} H.D. Wahl \ddagger^{97} R. Wallny $\dagger j^{15}$ M.H.L.S. Wang \ddagger^{15} S.M. Wang \dagger^1 J. Warchol \ddagger^{103} D. Waters \dagger^{28}
G. Watts \ddagger^{123} M. Wayne \ddagger^{103} J. Weichert \ddagger^{76} L. Welty-Rieger \ddagger^{100} W.C. Wester III \dagger^{15} D. Whiteson $\dagger c^{40}$
A.B. Wicklund \dagger^2 S. Wilbur \dagger^7 H.H. Williams \dagger^{40} M.R.J. Williams $\ddagger ww^{101}$ G.W. Wilson \ddagger^{105} J.S. Wilson \dagger^{31}
P. Wilson \dagger^{15} B.L. Winer \dagger^{35} P. Wittich $\dagger f^{15}$ M. Wobisch \ddagger^{106} S. Wolbers \dagger^{15} H. Wolfe \dagger^{35} D.R. Wood \ddagger^{107}
T. Wright \dagger^{31} X. Wu \dagger^{18} Z. Wu \dagger^5 T.R. Wyatt \ddagger^{94} Y. Xie \ddagger^{15} R. Yamada \ddagger^{15} K. Yamamoto \dagger^{37} D. Yamato \dagger^{37}
S. Yang \ddagger^{59} T. Yang \dagger^{15} U.K. Yang \dagger^{25} Y.C. Yang \dagger^{25} W.-M. Yao \dagger^{26} T. Yasuda \ddagger^{15} Y.A. Yatsunenko \ddagger^{13} W. Ye
 \ddagger^{113} Z. Ye \ddagger^{15} G.P. Yeh \dagger^{15} K. Yi $\dagger m^{15}$ H. Yin \ddagger^{15} K. Yip \ddagger^{114} J. Yoh \dagger^{15} K. Yorita \dagger^{52} T. Yoshida $\dagger k^{37}$
S.W. Youn \ddagger^{15} G.B. Yu \dagger^{14} I. Yu \dagger^{25} J.M. Yu \ddagger^{31} A.M. Zanetti \dagger^{48} Y. Zeng \dagger^{14} J. Zennamo \ddagger^{112} T.G. Zhao \ddagger^{94}
B. Zhou \ddagger^{31} C. Zhou \dagger^{14} J. Zhu \ddagger^{31} M. Zielinski \ddagger^{44} D. Ziemska \ddagger^{101} L. Zivkovic \ddagger^{69} and S. Zucchelli $\dagger xx^{6}$
(CDF Collaboration) $\cdot\dagger$
(D0 Collaboration) $\cdot\ddagger$

¹*Institute of Physics, Academia Sinica, Taipei, Taiwan 11529, Republic of China*

²*Argonne National Laboratory, Argonne, Illinois 60439, USA*

³*University of Athens, 157 71 Athens, Greece*

⁴*Institut de Fisica d'Altes Energies, ICREA, Universitat Autonoma de Barcelona, E-08193, Bellaterra (Barcelona), Spain*

⁵*Baylor University, Waco, Texas 76798, USA*

⁶*Istituto Nazionale di Fisica Nucleare Bologna, ^{xx}University of Bologna, I-40127 Bologna, Italy*

⁷*University of California, Davis, Davis, California 95616, USA*

⁸*University of California, Los Angeles, Los Angeles, California 90024, USA*

⁹*Instituto de Fisica de Cantabria, CSIC-University of Cantabria, 39005 Santander, Spain*

¹⁰*Carnegie Mellon University, Pittsburgh, Pennsylvania 15213, USA*

¹¹*Enrico Fermi Institute, University of Chicago, Chicago, Illinois 60637, USA*

¹²*Comenius University, 842 48 Bratislava, Slovakia; Institute of Experimental Physics, 040 01 Kosice, Slovakia*

¹³*Joint Institute for Nuclear Research, RU-141980 Dubna, Russia*

¹⁴*Duke University, Durham, North Carolina 27708, USA*

¹⁵*Fermi National Accelerator Laboratory, Batavia, Illinois 60510, USA*

¹⁶*University of Florida, Gainesville, Florida 32611, USA*

¹⁷*Laboratori Nazionali di Frascati, Istituto Nazionale di Fisica Nucleare, I-00044 Frascati, Italy*

¹⁸*University of Geneva, CH-1211 Geneva 4, Switzerland*

¹⁹*Glasgow University, Glasgow G12 8QQ, United Kingdom*

²⁰*Harvard University, Cambridge, Massachusetts 02138, USA*

²¹*Division of High Energy Physics, Department of Physics, University of Helsinki, FIN-00014, Helsinki, Finland*

²²*University of Illinois, Urbana, Illinois 61801, USA*

²³*The Johns Hopkins University, Baltimore, Maryland 21218, USA*

²⁴*Institut für Experimentelle Kernphysik, Karlsruhe Institute of Technology, D-76131 Karlsruhe, Germany*

²⁵*Center for High Energy Physics: Kyungpook National University,*

Daegu 702-701, Korea; Seoul National University, Seoul 151-742,

Korea; Sungkyunkwan University, Suwon 440-746,

Korea; Korea Institute of Science and Technology Information,

Daejeon 305-806, Korea; Chonnam National University,

Gwangju 500-757, Korea; Chonbuk National University, Jeonju 561-756,

Korea; Ewha Womans University, Seoul, 120-750, Korea

²⁶*Ernest Orlando Lawrence Berkeley National Laboratory, Berkeley, California 94720, USA*

²⁷*University of Liverpool, Liverpool L69 7ZE, United Kingdom*

²⁸*University College London, London WC1E 6BT, United Kingdom*

²⁹*Centro de Investigaciones Energeticas Medioambientales y Tecnologicas, E-28040 Madrid, Spain*

³⁰*Massachusetts Institute of Technology, Cambridge, Massachusetts 02139, USA*

³¹*University of Michigan, Ann Arbor, Michigan 48109, USA*

³²*Michigan State University, East Lansing, Michigan 48824, USA*

³³*Institution for Theoretical and Experimental Physics, ITEP, Moscow 117259, Russia*

³⁴*University of New Mexico, Albuquerque, New Mexico 87131, USA*

- ³⁵*The Ohio State University, Columbus, Ohio 43210, USA*
³⁶*Okayama University, Okayama 700-8530, Japan*
³⁷*Osaka City University, Osaka 558-8585, Japan*
³⁸*University of Oxford, Oxford OX1 3RH, United Kingdom*
- ³⁹*Istituto Nazionale di Fisica Nucleare, Sezione di Padova, ⁴⁰University of Padova, I-35131 Padova, Italy*
⁴⁰*University of Pennsylvania, Philadelphia, Pennsylvania 19104, USA*
⁴¹*Istituto Nazionale di Fisica Nucleare Pisa, ⁴²University of Pavia, I-27100 Pavia, Italy*
⁴²*University of Siena, Scuola Normale Superiore, I-56127 Pisa, Italy, INFN Pavia, I-27100 Pavia, Italy*
⁴³*Purdue University, West Lafayette, Indiana 47907, USA*
⁴⁴*University of Rochester, Rochester, New York 14627, USA*
⁴⁵*The Rockefeller University, New York, New York 10065, USA*
⁴⁶*Istituto Nazionale di Fisica Nucleare, Sezione di Roma 1, Sapienza Università di Roma, I-00185 Roma, Italy*
⁴⁷*Mitchell Institute for Fundamental Physics and Astronomy, Texas A&M University, College Station, Texas 77843, USA*
- ⁴⁸*Istituto Nazionale di Fisica Nucleare Trieste, Gruppo Collegato di Udine, University of Udine, I-33100 Udine, Italy, University of Trieste, I-34127 Trieste, Italy*
⁴⁹*University of Tsukuba, Tsukuba, Ibaraki 305, Japan*
⁵⁰*Tufts University, Medford, Massachusetts 02155, USA*
⁵¹*University of Virginia, Charlottesville, Virginia 22906, USA*
⁵²*Waseda University, Tokyo 169, Japan*
⁵³*Wayne State University, Detroit, Michigan 48201, USA*
⁵⁴*University of Wisconsin, Madison, Wisconsin 53706, USA*
⁵⁵*Yale University, New Haven, Connecticut 06520, USA*
- ⁵⁶*LAFEX, Centro Brasileiro de Pesquisas Físicas, Rio de Janeiro, Brazil*
⁵⁷*Universidade do Estado do Rio de Janeiro, Rio de Janeiro, Brazil*
⁵⁸*Universidade Federal do ABC, Santo André, Brazil*
- ⁵⁹*University of Science and Technology of China, Hefei, People's Republic of China*
⁶⁰*Universidad de los Andes, Bogotá, Colombia*
- ⁶¹*Charles University, Faculty of Mathematics and Physics, Center for Particle Physics, Prague, Czech Republic*
⁶²*Czech Technical University in Prague, Prague, Czech Republic*
- ⁶³*Institute of Physics, Academy of Sciences of the Czech Republic, Prague, Czech Republic*
⁶⁴*Universidad San Francisco de Quito, Quito, Ecuador*
- ⁶⁵*LPC, Université Blaise Pascal, CNRS/IN2P3, Clermont, France*
⁶⁶*LPSC, Université Joseph Fourier Grenoble 1, CNRS/IN2P3, Institut National Polytechnique de Grenoble, Grenoble, France*
⁶⁷*CPPM, Aix-Marseille Université, CNRS/IN2P3, Marseille, France*
⁶⁸*LAL, Université Paris-Sud, CNRS/IN2P3, Orsay, France*
- ⁶⁹*LPNHE, Universités Paris VI and VII, CNRS/IN2P3, Paris, France*
⁷⁰*CEA, Irfu, SPP, Saclay, France*
- ⁷¹*IPHC, Université de Strasbourg, CNRS/IN2P3, Strasbourg, France*
- ⁷²*IPNL, Université Lyon 1, CNRS/IN2P3, Villeurbanne, France and Université de Lyon, Lyon, France*
- ⁷³*III. Physikalisches Institut A, RWTH Aachen University, Aachen, Germany*
⁷⁴*Physikalisches Institut, Universität Freiburg, Freiburg, Germany*
- ⁷⁵*II. Physikalisches Institut, Georg-August-Universität Göttingen, Göttingen, Germany*
⁷⁶*Institut für Physik, Universität Mainz, Mainz, Germany*
⁷⁷*Ludwig-Maximilians-Universität München, München, Germany*
⁷⁸*Panjab University, Chandigarh, India*
⁷⁹*Delhi University, Delhi, India*
- ⁸⁰*Tata Institute of Fundamental Research, Mumbai, India*
⁸¹*University College Dublin, Dublin, Ireland*
- ⁸²*Korea Detector Laboratory, Korea University, Seoul, Korea*
⁸³*CINVESTAV, Mexico City, Mexico*
- ⁸⁴*Nikhef, Science Park, Amsterdam, the Netherlands*
⁸⁵*Radboud University Nijmegen, Nijmegen, the Netherlands*
⁸⁶*Moscow State University, Moscow, Russia*
- ⁸⁷*Institute for High Energy Physics, Protvino, Russia*
⁸⁸*Petersburg Nuclear Physics Institute, St. Petersburg, Russia*
- ⁸⁹*Institució Catalana de Recerca i Estudis Avançats (ICREA) and Institut de Física d'Altes Energies (IFAE), Barcelona, Spain*
⁹⁰*Uppsala University, Uppsala, Sweden*

- ⁹¹*Taras Shevchenko National University of Kyiv, Kiev, Ukraine*
⁹²*Lancaster University, Lancaster LA1 4YB, United Kingdom*
⁹³*Imperial College London, London SW7 2AZ, United Kingdom*
⁹⁴*The University of Manchester, Manchester M13 9PL, United Kingdom*
⁹⁵*University of Arizona, Tucson, Arizona 85721, USA*
⁹⁶*University of California Riverside, Riverside, California 92521, USA*
⁹⁷*Florida State University, Tallahassee, Florida 32306, USA*
⁹⁸*University of Illinois at Chicago, Chicago, Illinois 60607, USA*
⁹⁹*Northern Illinois University, DeKalb, Illinois 60115, USA*
¹⁰⁰*Northwestern University, Evanston, Illinois 60208, USA*
¹⁰¹*Indiana University, Bloomington, Indiana 47405, USA*
¹⁰²*Purdue University Calumet, Hammond, Indiana 46323, USA*
¹⁰³*University of Notre Dame, Notre Dame, Indiana 46556, USA*
¹⁰⁴*Iowa State University, Ames, Iowa 50011, USA*
¹⁰⁵*University of Kansas, Lawrence, Kansas 66045, USA*
¹⁰⁶*Louisiana Tech University, Ruston, Louisiana 71272, USA*
¹⁰⁷*Northeastern University, Boston, Massachusetts 02115, USA*
¹⁰⁸*University of Mississippi, University, Mississippi 38677, USA*
¹⁰⁹*University of Nebraska, Lincoln, Nebraska 68588, USA*
¹¹⁰*Rutgers University, Piscataway, New Jersey 08855, USA*
¹¹¹*Princeton University, Princeton, New Jersey 08544, USA*
¹¹²*State University of New York, Buffalo, New York 14260, USA*
¹¹³*State University of New York, Stony Brook, New York 11794, USA*
¹¹⁴*Brookhaven National Laboratory, Upton, New York 11973, USA*
¹¹⁵*Langston University, Langston, Oklahoma 73050, USA*
¹¹⁶*University of Oklahoma, Norman, Oklahoma 73019, USA*
¹¹⁷*Oklahoma State University, Stillwater, Oklahoma 74078, USA*
¹¹⁸*Brown University, Providence, Rhode Island 02912, USA*
¹¹⁹*University of Texas, Arlington, Texas 76019, USA*
¹²⁰*Southern Methodist University, Dallas, Texas 75275, USA*
¹²¹*Rice University, Houston, Texas 77005, USA*
¹²²*University of Virginia, Charlottesville, Virginia 22904, USA*
¹²³*University of Washington, Seattle, Washington 98195, USA*

(Dated: February 3, 2015)

Combined constraints from the CDF and D0 Collaborations on models of the Higgs boson with exotic spin J and parity P are presented and compared with results obtained assuming the standard model value $J^P = 0^+$. Both collaborations analyzed approximately 10 fb^{-1} of proton-antiproton collisions with a center-of-mass energy of 1.96 TeV collected at the Fermilab Tevatron. Two models predicting exotic Higgs bosons with $J^P = 0^-$ and $J^P = 2^+$ are tested. The kinematic properties of exotic Higgs boson production in association with a vector boson differ from those predicted for the standard model Higgs boson. Upper limits at the 95% credibility level on the production rates of the exotic Higgs bosons, expressed as fractions of the standard model Higgs boson production rate, are set at 0.36 for both the $J^P = 0^-$ hypothesis and the $J^P = 2^+$ hypothesis. If the production rate times the branching ratio to a bottom-antibottom pair is the same as that predicted for the standard model Higgs boson, then the exotic bosons are excluded with significances of 5.0 standard deviations and 4.9 standard deviations for the $J^P = 0^-$ and $J^P = 2^+$ hypotheses, respectively.

PACS numbers: 13.85.Rm, 14.80.Bn, 14.80.Ec

The Higgs boson discovered by the ATLAS [1] and CMS [2] Collaborations in 2012 using data produced in proton-proton collisions at the Large Hadron Collider (LHC) at CERN allows many stringent tests of the electroweak symmetry breaking in the standard model (SM) and extensions to the SM to be performed. To date, measurements of the Higgs boson's mass and width [3–6], its couplings to other particles [3, 7–11], and its spin and parity quantum numbers J and P [10–16] are consistent with the expectations for the SM Higgs boson. The CDF and D0 Collaborations at the Fermilab Tevatron observed a 3.0 standard deviation (s.d.) excess of events

consistent with a Higgs boson signal, largely driven by those channels sensitive to the decay of the Higgs boson to bottom quarks ($H \rightarrow b\bar{b}$) [17, 18]. The Tevatron data are also consistent with the predictions for the properties of the SM Higgs boson [18–22].

Ref. [23] proposed to use the Tevatron data to test models for the Higgs boson with exotic spin and parity, using events in which the exotic Higgs boson X is produced in association with a W or a Z boson and decays to a bottom-antibottom quark pair, $X \rightarrow b\bar{b}$. This proposal used two of the spin and parity models in Ref. [24], one with a pseudoscalar $J^P = 0^-$ state and the other with

a graviton-like $J^P = 2^+$ state. For the SM Higgs boson, which has $J^P = 0^+$, the differential production rate near threshold is linear in β , where $\beta = 2p/\sqrt{s}$, p is the momentum of the X boson in the VX ($V = W$ or Z) reference frame, and \sqrt{s} is the total energy of the VX system in its rest frame. For the pseudoscalar model, the dependence is proportional to β^3 . For the graviton-like model, the dependence is proportional to β^5 ; however, not all $J^P = 2^+$ models share this β^5 factor [23]. These powers of β alter the kinematic distributions of the observable decay products of the vector boson and the Higgs-like boson X , most notably the invariant mass of the VX system, which has a higher average value in the $J^P = 0^-$ hypothesis than in the SM 0^+ case, and higher still in the $J^P = 2^+$ hypothesis. These models predict neither the production rates nor the decay branching fractions of the X particles.

The ATLAS and CMS Collaborations recently reported strong evidence for Higgs boson decays to fermions [25–30], with sensitivity dominated by the $H \rightarrow \tau^+\tau^-$ decay mode, though they have not yet performed spin and parity tests using fermionic decays. The particle decaying fermionically for which the Tevatron also found evidence might not be the same as the particle discovered through its bosonic decays at the LHC. Tests of the spin and parity [23] with Tevatron data therefore provide unique information on the identity and properties of the new particle or particles. The CDF and D0 Collaborations have re-optimized their SM Higgs boson searches to test the exotic Higgs boson models in the $WH \rightarrow \ell\nu b\bar{b}$ [31, 32], $ZH \rightarrow \ell^+\ell^-\bar{b}\bar{b}$ [33, 34], and $WH + ZH \rightarrow \cancel{E}_T b\bar{b}$ [35, 36] channels, where $\ell = e$ or μ and \cancel{E}_T is the missing transverse energy [37]. In this letter we report a combination of the CDF [21] and D0 [22] studies of the J^P assignments of the state X , with mass $m_X = 125$ GeV/ c^2 , in the $X \rightarrow b\bar{b}$ decay.

The CDF and D0 detectors are multipurpose solenoidal spectrometers surrounded by hermetic calorimeters and muon detectors designed to study the products of 1.96 TeV proton-antiproton ($p\bar{p}$) collisions [38, 39]. All searches combined here use the complete Tevatron data sample, which, after data quality requirements, corresponds to $9.45 - 9.7$ fb $^{-1}$ of integrated luminosity, depending on the experiment and the search channel.

Standard model Higgs boson signal events are simulated using the leading-order (LO) calculation from PYTHIA [40], with CTEQ5L (CDF) and CTEQ6L1 (D0) [41] parton distribution functions (PDFs). The $J^P = 0^-$ and $J^P = 2^+$ signal samples are generated using MADGRAPH 5 version 1.4.8.4 [42], with modifications provided by the authors of Ref. [23]. Subsequent particle showering is modeled by PYTHIA. We normalize the SM Higgs boson rate predictions to the highest-order calculations available. The WH and ZH cross sections are calculated at next-to-next-to-leading-order (NNLO) precision in the strong interaction, and next-to-leading-order

(NLO) precision in the electroweak corrections [43–46]. We use the branching fractions for Higgs boson decay from Ref. [47]. These rely on calculations using HDECAY [48] and PROPHECY4F [49].

The predictions of the dominant background rates and kinematic distributions are treated in the following way. Diboson (WW , WZ , and ZZ) Monte Carlo (MC) samples are normalized using the NLO calculations from MCFM [50]. For $t\bar{t}$, we use a production cross section of 7.04 ± 0.70 pb [51], which is based on a top quark mass of 173 GeV/ c^2 [52] and MSTW 2008 NNLO PDFs [53]. The single top quark production cross section is assumed to be 3.15 ± 0.31 pb [54]. For details of the generators used, see Ref. [55]. Data-driven methods are used to normalize the V plus light-flavor and heavy-flavor jet backgrounds [60] using V data events containing no b -tagged jets [61], which have negligible signal content [62, 63]. The MC modeling of the kinematic distributions of the background predictions is described in Refs. [31–36].

The event selections are similar (CDF), or identical (D0), to those used in their SM counterparts [31–36]. For the $WH \rightarrow \ell\nu b\bar{b}$ analyses, events are selected with one identified lepton (e or μ), jets, and large \cancel{E}_T . For the CDF $WH \rightarrow \ell\nu b\bar{b}$ analysis, only events with two jets are used. Events are classified into separate categories based on the quality of the identified lepton. Separate categories are used for events with a high-quality muon or central electron candidate, an isolated track, or a forward electron candidate. Within the lepton categories, five exclusive b -tag categories, comprising two single-tag and three double-tag categories, are formed. The multivariate b -tagger used by CDF [64] was trained on SM Higgs boson signal MC events. Few of these events contained jets with transverse energy $E_T > 200$ GeV and thus the tagger does not perform well for such jets. Hence, only jets with $E_T < 200$ GeV are considered. For the D0 $WH \rightarrow \ell\nu b\bar{b}$ analysis, events are selected with two or three jets. The data are split by lepton flavor and jet multiplicity (two or three jet subchannels), and by the output of the b -tagging algorithm applied to all selected jets in the event. This channel, along with the other two D0 channels, uses a multivariate b -tagging algorithm [65, 66]. Four exclusive b -tag categories, one single-tag and three double-tag, are formed. In the SM Higgs boson search, boosted decision trees are used as the final discriminating variables; here they are used to further subdivide the selected data sample into high- and low-purity categories.

The $ZH \rightarrow \ell^+\ell^-\bar{b}\bar{b}$ analyses require two isolated leptons and at least two jets. The CDF analysis separates events into one single- and three double- b -tag samples and uses neural networks to select loose dielectron and dimuon candidates. The jet energies are corrected for \cancel{E}_T using a neural network [67]. The CDF analysis uses a multistep discriminant based on neural networks, where two discriminant functions are used to define three sep-

arate regions of the final discriminant function. The D0 $ZH \rightarrow \ell^+ \ell^- b\bar{b}$ analysis separates events into non-overlapping samples of events with either a single or double b -tag. To increase the signal acceptance, the selection criteria for one of the leptons are loosened to include isolated tracks not reconstructed in the muon detector and electron candidates from the intercryostat region of the D0 detector. Combined with the dielectron and dimuon categories, these provide four independent lepton subchannels. A kinematic fit is used to optimize reconstruction. Random forests (RF) of decision trees [68, 69] are used to provide the final variables in the SM Higgs boson search. The first RF is designed to discriminate against $t\bar{t}$ events and divides events into $t\bar{t}$ -enriched and $t\bar{t}$ -depleted single-tag and double-tag regions. Only events in the $t\bar{t}$ -depleted regions are considered in this study. These regions contain approximately 94% of the SM signal.

For the $ZH \rightarrow \nu\bar{\nu}b\bar{b}$ analyses, the selections used by CDF and D0 are similar to the WH selections, except that all events with isolated leptons are rejected and more stringent techniques are applied to reject the multijet background. In a sizable fraction of $WH \rightarrow \ell\nu b\bar{b}$ signal events, the lepton is undetected. Such events often are selected in the $ZH \rightarrow \nu\bar{\nu}b\bar{b}$ samples, so these analyses are also referred to as $VH \rightarrow \cancel{E}_T b\bar{b}$. The CDF analysis uses three non-overlapping b -tag categories (two double- and one single-tag) and two jet categories (two- or three-jet events), giving a total of six subchannels. In the D0 analysis, exactly two jets are required and two exclusive double-tag categories are defined using the sum of the b -tagging outputs for each of the two selected jets.

Both CDF and D0 have a 50% larger acceptance for the $J^P = 0^-$ and $J^P = 2^+$ signals in the $ZH \rightarrow \nu\bar{\nu}b\bar{b}$ analyses compared with the SM Higgs boson signal, largely due to the fact that the exotic signal events are more likely to pass the trigger thresholds for \cancel{E}_T , a consequence of the larger average VX invariant masses. The other two channels, $WH \rightarrow \ell\nu b\bar{b}$ and $ZH \rightarrow \ell^+ \ell^- b\bar{b}$, do not benefit as much from the additional \cancel{E}_T in these events, as they rely on the lepton triggers, which are more efficient than the \cancel{E}_T triggers in the relevant kinematic regions.

Unlike their SM counterparts, these analyses are optimized to distinguish the $J^P = 0^-$ and the $J^P = 2^+$ hypotheses from the SM 0^+ hypothesis. The exotic particles are considered either in addition to, or replacing, the SM Higgs boson. A mixture of all three states is not considered.

The CDF multivariate analysis (MVA) discriminants were newly trained to separate the exotic Higgs boson signals from the SM backgrounds [21]. In the $WH \rightarrow \ell\nu b\bar{b}$ and $VH \rightarrow \cancel{E}_T b\bar{b}$ channels, events classified as background-like by the new discriminants are then classified according to the SM-optimized MVA discriminants in order to improve the performance of tests between the SM and exotic hypotheses.

Depending on the channel, D0 uses either the recon-

structed dijet mass or the MVA used in the SM Higgs boson search to separate events into high- and low-purity samples. The mass of the VX system is then used to discriminate between the exotic and SM hypotheses [22]. For the $ZH \rightarrow \ell\ell b\bar{b}$ analysis the invariant mass of the two leptons and the two highest p_T jets is used. For the $\ell\nu b\bar{b}$ and $\nu\nu b\bar{b}$ final states the transverse mass M_T is used, where $M_T^2 = (E_T^V + E_T^X)^2 - (\vec{p}_T^V + \vec{p}_T^X)^2$ and the transverse momenta of the Z and W bosons are taken to be $\vec{p}_T^Z = \vec{\cancel{E}}_T$ and $\vec{p}_T^W = \vec{\cancel{E}}_T + \vec{p}_T^\ell$, respectively.

The number of contributing channels is large, and their sensitivities vary from one to another. To visualize the data in a way that emphasizes the sensitivity to the exotic signals, we follow Ref. [18]. Bins of the final discriminant for all channels are ordered by increasing signal-to-background ratio (s/b) and are shown in comparison with predicted yields from signal and background processes for the $J^P = 0^-$ and $J^P = 2^+$ searches in Fig. 1 separately. The backgrounds are fit to the data in each case, allowing the systematic uncertainties to vary within their a priori constraints. The exotic signals are normalized to the SM cross section times branching ratio multiplied by an exotic-signal scaling factor, μ_{exotic} . They are shown in Fig. 1 with $\mu_{\text{exotic}} = 1$. The scaling factor for the SM Higgs boson signal is denoted by μ_{SM} . A value of one for either μ_{SM} or μ_{exotic} corresponds to a cross section times branching ratio as predicted for the SM Higgs boson. Both figures show agreement between the background predictions and the observed data over five orders of magnitude with no evidence for an excess of exotic signal-like candidates.

We follow Ref. [18] and perform both Bayesian and modified frequentist calculations of the upper limits on exotic X boson production with and without SM Higgs production, best-fit cross sections allowing for the simultaneous presence of a SM Higgs boson and an exotic X boson, and hypothesis tests for signals assuming various production rate times branching ratio values for the exotic bosons. Both methods use likelihood calculations based on Poisson probabilities that include SM background processes and signal predictions for the SM Higgs and exotic bosons multiplied by their respective scaling factors, μ_{SM} and μ_{exotic} . Systematic uncertainties on the predicted rates and on the shapes of the distributions and their correlations are treated as described in Ref. [18]. Theoretical uncertainties in cross sections and branching ratios are considered fully correlated between CDF and D0, and between analysis samples. The uncertainties on the measurements of the integrated luminosities, which are used to normalize the expected signal yields and the MC-based background rates, are 6.0% (CDF) and 6.1% (D0). Of these values, 4% arises from the inelastic $p\bar{p}$ cross section [70], which is fully correlated between CDF and D0. The dominant uncertainties on the backgrounds are constrained by the data in low s/b regions of the discriminant distributions. Different methods were used

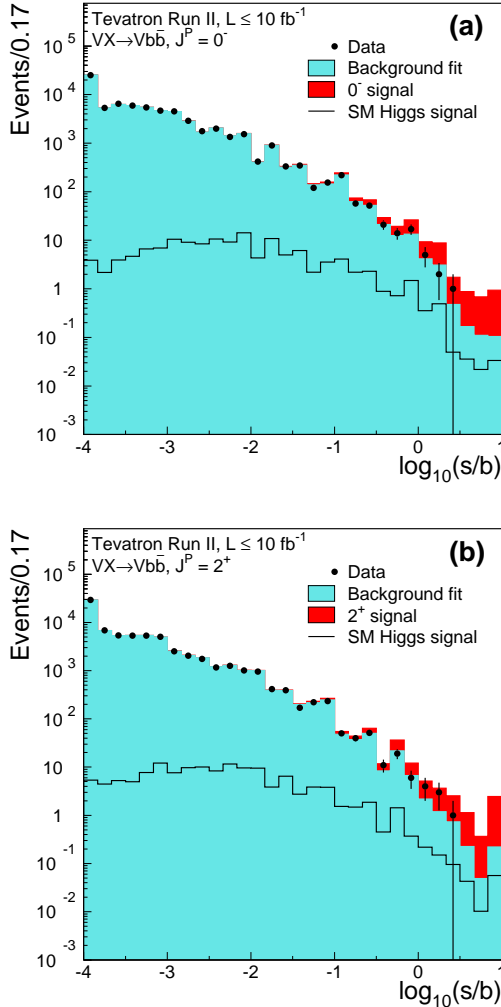


FIG. 1: (color online). Distribution of $\log_{10}(s/b)$ for CDF and D0 data from all contributing search channels, for (a) the $J^P = 0^-$ search and (b) the $J^P = 2^+$ search. The data are shown with points, and the expected exotic signals are shown with $\mu_{\text{exotic}} = 1$ stacked on top of the fitted backgrounds. The solid lines denote the predictions for the SM Higgs boson, and are not stacked. Underflows and overflows are collected into the leftmost and rightmost bins, respectively.

by CDF and D0 to estimate $V+\text{jets}$ and multijet backgrounds and so their uncertainties are considered uncorrelated. Similarly, the uncertainties on the data-driven estimates of the b -tag efficiencies are considered uncorrelated between CDF and D0, as are the uncertainties on the jet energy scales, the trigger efficiencies, and lepton identification efficiencies. We quote Bayesian upper limits and best-fit cross sections assuming uniform priors for non-negative signal cross sections, and we use the modified frequentist method to perform the hypothesis tests. Systematic uncertainties are parameterized by nuisance parameters with Gaussian priors, truncated so that no predicted yield for any process in any search channel is

negative.

For both the $J^P = 0^-$ and $J^P = 2^+$ models, we compute two 95% credibility upper limits on μ_{exotic} , one assuming $\mu_{\text{SM}} = 1$ and the other assuming $\mu_{\text{SM}} = 0$. The expected limits are the median expectations assuming no exotic boson is present. The results are listed in Table I. Two-dimensional credibility regions, which are the smallest regions containing 68% and 95% of the posterior probabilities, are shown in Fig. 2. The points in the $(\mu_{\text{SM}}, \mu_{\text{exotic}})$ planes that maximize the posterior probability densities are shown as the best-fit values. These best-fit values are $(\mu_{\text{SM}}=1.0, \mu_{0^-}=0)$ for the search for the $J^P = 0^-$ state, and $(\mu_{\text{SM}}=1.1, \mu_{2^+}=0)$ for the search for the $J^P = 2^+$ state. We also derive upper limits on the fraction $f_{JP} = \mu_{\text{exotic}} / (\mu_{\text{exotic}} + \mu_{\text{SM}})$, as functions of the total $\mu = \mu_{\text{exotic}} + \mu_{\text{SM}}$, assuming a uniform prior probability density in non-negative f_{JP} , extended to include fractions larger than 1.0 in order not to saturate the limits at $f_{JP} = 0.95$ for $\mu < 0.6$, where the test is weak. The results are shown in Fig. 3.

In the modified frequentist approach [71, 72] we compute p values for the discrete two-hypothesis tests, the SM Higgs boson hypothesis (the “null” hypothesis) ($\mu_{\text{SM}}=1, \mu_{\text{exotic}}=0$) and the exotic (“test”) hypothesis ($\mu_{\text{SM}}=0, \mu_{\text{exotic}}=1$), both assuming that SM background processes are present. The choice of setting $\mu_{\text{exotic}} = 1$ in the test hypothesis is arbitrary; the sensitivity of the test is reduced if a smaller value is assumed. We use the log-likelihood ratio, LLR, defined to be $-2 \ln(p(\text{data|test})/p(\text{data|null}))$, where the numerator and denominator are maximized over systematic uncertainty variations [18]. The LLR distributions are shown in the supplemental material [73]. We define the p values $p_{\text{null}} = P(\text{LLR} \leq \text{LLR}_{\text{obs}}|\text{SM})$ and $p_{\text{test}} = P(\text{LLR} \geq \text{LLR}_{\text{obs}}|\text{exotic})$. The median expected p values $p_{\text{null,med}}^{\text{exotic}}$ in the test hypothesis and $p_{\text{test,med}}^{\text{SM}}$ in the SM hypothesis quantify the sensitivities of the two-hypothesis tests for exclusion and discovery, respectively. Table II lists these p values for both exotic models, as well as $\text{CL}_s = p_{\text{test}} / (1 - p_{\text{null}})$ [71] for the Tevatron combination. To compute p_{test} and the expected values of p_{null} and p_{test} , Wilks’s theorem is used [74].

The similarity of the limits and p values obtained for the $J^P = 0^-$ and the $J^P = 2^+$ searches is expected since the exotic models predict excesses in similar portions of kinematic space.

In summary, we combine CDF’s and D0’s tests for the presence of a pseudoscalar Higgs boson with $J^P = 0^-$ and a graviton-like boson with $J^P = 2^+$ in the $WX \rightarrow \ell\nu b\bar{b}$, the $ZX \rightarrow \ell^+\ell^- b\bar{b}$, and the $VX \rightarrow \#_T b\bar{b}$ search channels using models described in Ref. [23]. The masses of the exotic bosons are assumed to be 125 GeV/ c^2 . No evidence is seen for either exotic particle, either in place of the SM Higgs boson or produced in a mixture with a $J^P = 0^+$ Higgs boson. In both searches, the best-fit cross section times the decay branching ratio into a bottom-

TABLE I: Observed and median expected Bayesian upper limits at the 95% credibility level on μ_{exotic} for the pseudoscalar ($J^P = 0^-$) and graviton-like ($J^P = 2^+$) boson models, assuming either that the SM Higgs boson is also present ($\mu_{\text{SM}} = 1$) or absent ($\mu_{\text{SM}} = 0$).

Channel	Observed (Limit/ σ_{SM})	Median Expected (Limit/ σ_{SM})
$J^P = 0^-, \mu_{\text{SM}} = 0$	0.36	0.32
$J^P = 0^-, \mu_{\text{SM}} = 1$	0.29	0.32
$J^P = 2^+, \mu_{\text{SM}} = 0$	0.36	0.33
$J^P = 2^+, \mu_{\text{SM}} = 1$	0.31	0.34

TABLE II: Observed (obs) and median expected (med) LLR values and p values for the combined CDF and D0 searches for the pseudoscalar ($J^P = 0^-$) boson and the graviton-like ($J^P = 2^+$) boson. The p values are listed, and the corresponding significances in units of standard deviations, using a one-sided Gaussian tail calculation, are given in parentheses. The two hypotheses tested are $(\mu_{\text{SM}}, \mu_{\text{exotic}}) = (1, 0)$ and $(0, 1)$ for the SM and the exotic models, respectively.

Analysis	$J^P = 0^-$	$J^P = 2^+$
LLR _{obs}	27.1	25.7
LLR _{med} SM	23.7	21.8
LLR _{med} ^{exotic}	-29.9	-29.6
p_{null}	0.63 (-0.34)	0.66 (-0.41)
$p_{\text{null,med}}^{\text{exotic}}$	1.8×10^{-8} (5.5)	1.9×10^{-8} (5.5)
p_{test}	9.4×10^{-8} (5.2)	1.9×10^{-7} (5.1)
$p_{\text{test,med}}^{\text{SM}}$	4.7×10^{-7} (4.9)	1.2×10^{-6} (4.7)
CL _s	2.6×10^{-7} (5.0)	5.6×10^{-7} (4.9)
CL _{s,med} SM	9.4×10^{-7} (4.8)	2.3×10^{-6} (4.6)

antibottom quark pair of a $J^P = 0^+$ signal component is consistent with the prediction of the SM Higgs boson. The Bayesian posterior probability densities for the $J^P = 0^-$ and $J^P = 2^+$ searches are shown in Ref. [73].

Upper limits at 95% credibility on the rate of the production of an exotic Higgs boson in the absence of a SM $J^P = 0^+$ signal are set at 0.36 times the SM Higgs production rate for both the $J^P = 0^-$ and the $J^P = 2^+$ hypotheses. If the production rate of the hypothetical exotic particle times its branching ratio to a bottom-antibottom quark pair is the same as that predicted for the SM Higgs boson, then the exotic models are excluded with significances of 5.0 s.d. and 4.9 s.d. for the $J^P = 0^-$ and $J^P = 2^+$ hypotheses, respectively.

Acknowledgments

We thank the Fermilab staff and technical staffs of the participating institutions for their vital contributions. We acknowledge support from the Department of Energy

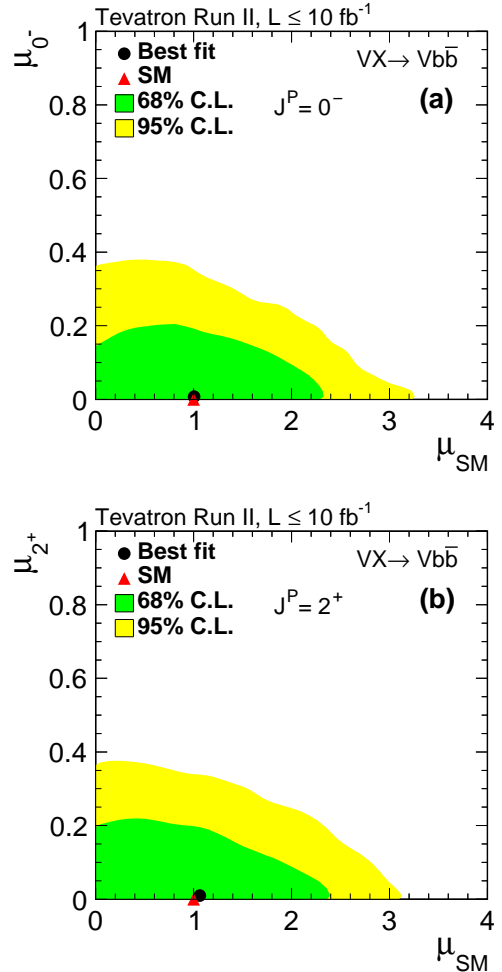


FIG. 2: (color online). Two-dimensional credibility regions in the $(\mu_{\text{exotic}}, \mu_{\text{SM}})$ plane, for the combined CDF and D0 searches for (a) the pseudoscalar ($J^P = 0^-$) boson, and (b) the graviton-like ($J^P = 2^+$) boson.

and the National Science Foundation (United States of America), the Australian Research Council (Australia), the National Council for the Development of Science and Technology and the Carlos Chagas Filho Foundation for the Support of Research in the State of Rio de Janeiro (Brazil), the Natural Sciences and Engineering Research Council (Canada), the China Academy of Sciences, the National Natural Science Foundation of China, and the National Science Council of the Republic of China (China), the Administrative Department of Science, Technology and Innovation (Colombia), the Ministry of Education, Youth and Sports (Czech Republic), the Academy of Finland (Finland), the Alternative Energies and Atomic Energy Commission and the National Center for Scientific Research/National Institute of Nuclear and Particle Physics (France), the Bundesministerium für Bildung und Forschung (Federal

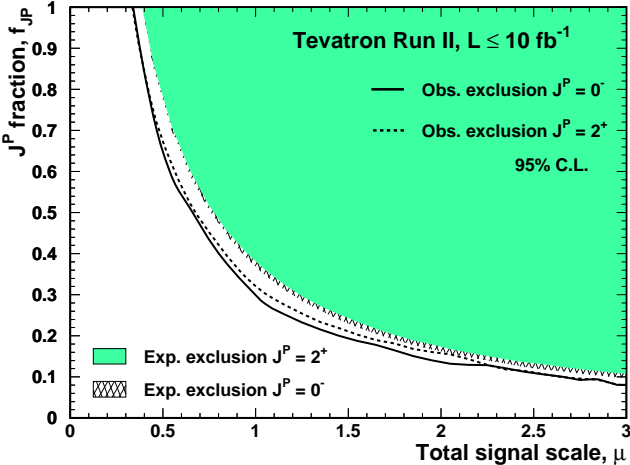


FIG. 3: (color online). Observed and expected upper limits at the 95% C.L. on the fraction of exotic boson production for the $J^P = 0^-$ and $J^P = 2^+$ hypotheses.

Ministry of Education and Research) and the Deutsche Forschungsgemeinschaft (German Research Foundation) (Germany), the Department of Atomic Energy and Department of Science and Technology (India), the Science Foundation Ireland (Ireland), the National Institute for Nuclear Physics (Italy), the Ministry of Education, Culture, Sports, Science and Technology (Japan), the Korean World Class University Program and the National Research Foundation of Korea (Korea), the National Council of Science and Technology (Mexico), the Foundation for Fundamental Research on Matter (Netherlands), the Ministry of Education and Science of the Russian Federation, the National Research Center “Kurchatov Institute” of the Russian Federation, and the Russian Foundation for Basic Research (Russia), the Slovak R&D Agency (Slovakia), the Ministry of Science and Innovation, and the Consolider-Ingenio 2010 Program (Spain), the Swedish Research Council (Sweden), the Swiss National Science Foundation (Switzerland), the Ministry of Education and Science of Ukraine (Ukraine), the Science and Technology Facilities Council and The Royal Society (United Kingdom), the A.P. Sloan Foundation (USA), and the European Union community Marie Curie Fellowship contract 302103.

versity, Ithaca, NY 14853, USA, ^gUniversity of Cyprus, Nicosia CY-1678, Cyprus, ^hOffice of Science, U.S. Department of Energy, Washington, DC 20585, USA, ⁱUniversity College Dublin, Dublin 4, Ireland, ^jETH, 8092 Zürich, Switzerland, ^kUniversity of Fukui, Fukui City, Fukui Prefecture, Japan 910-0017, ^lUniversidad Iberoamericana, Lomas de Santa Fe, México, C.P. 01219, Distrito Federal, ^mUniversity of Iowa, Iowa City, IA 52242, USA, ⁿKinki University, Higashi-Osaka City, Japan 577-8502, ^oKansas State University, Manhattan, KS 66506, USA, ^pBrookhaven National Laboratory, Upton, NY 11973, USA, ^qIstituto Nazionale di Fisica Nucleare, Sezione di Lecce, Via Arnesano, I-73100 Lecce, Italy, ^rQueen Mary, University of London, London, E1 4NS, United Kingdom, ^sUniversity of Melbourne, Victoria 3010, Australia, ^tMuons, Inc., Batavia, IL 60510, USA, ^uNagasaki Institute of Applied Science, Nagasaki 851-0193, Japan, ^vNational Research Nuclear University, Moscow 115409, Russia, ^wNorthwestern University, Evanston, IL 60208, USA, ^xUniversity of Notre Dame, Notre Dame, IN 46556, USA, ^yUniversidad de Oviedo, E-33007 Oviedo, Spain, ^zCNRS-IN2P3, Paris, F-75205 France, ^{aa}Universidad Técnica Federico Santa María, 110v Valparaíso, Chile, ^{bb}The University of Jordan, Amman 11942, Jordan, ^{cc}Université catholique de Louvain, 1348 Louvain-La-Neuve, Belgium, ^{dd}University of Zürich, 8006 Zürich, Switzerland, ^{ee}Massachusetts General Hospital, Boston, MA 02114 USA, ^{ff}Harvard Medical School, Boston, MA 02114 USA, ^{gg}Hampton University, Hampton, VA 23668, USA, ^{hh}Los Alamos National Laboratory, Los Alamos, NM 87544, USA, ⁱⁱUniversità degli Studi di Napoli Federico I, I-80138 Napoli, Italy

[†] With visitors from ^{jj}Augustana College, Sioux Falls, SD, USA, ^{kk}The University of Liverpool, Liverpool, UK, ^{ll}DESY, Hamburg, Germany, ^{mm}Universidad Michoacana de San Nicolas de Hidalgo, Morelia, Mexico, ⁿⁿSLAC, Menlo Park, CA, USA, ^{oo}University College London, London, UK, ^{pp}Centro de Investigacion en Computacion - IPN, Mexico City, Mexico, ^{qq}Universidade Estadual Paulista, São Paulo, Brazil, ^{rr}Karlsruher Institut für Technologie (KIT) - Steinbuch Centre for Computing (SCC), ^{ss}Office of Science, U.S. Department of Energy, Washington, D.C. 20585, USA, ^{tt}American Association for the Advancement of Science, Washington, D.C. 20005, USA, ^{uu}National Academy of Science of Ukraine (NASU) - Kiev Institute for Nuclear Research (KINR), ^{vv}University of Maryland, College Park, MD 20742, ^{ww}European Organization for Nuclear Research (CERN)

- [1] G. Aad *et al.* (ATLAS Collaboration), Phys. Lett. B **716**, 1 (2012).
- [2] S. Chatrchyan *et al.* (CMS Collaboration), Phys. Lett. B **716**, 30 (2012).
- [3] S. Chatrchyan *et al.* (CMS Collaboration), J. High Energy Phys. 06 (2013) 081.
- [4] G. Aad *et al.* (ATLAS Collaboration), Phys. Rev. D **90**, 052004 (2014).
- [5] G. Aad *et al.* (ATLAS Collaboration), ATLAS-CONF-2014-042 (2014).
- [6] S. Chatrchyan *et al.* (CMS Collaboration), Phys. Lett. B **736**, 64 (2014).
- [7] G. Aad *et al.* (ATLAS Collaboration), Phys. Lett. B **726**, 88 (2013).
- [8] G. Aad *et al.* (ATLAS Collaboration), ATLAS-CONF-

* Deceased

[†] With visitors from ^aUniversity of British Columbia, Vancouver, BC V6T 1Z1, Canada, ^bIstituto Nazionale di Fisica Nucleare, Sezione di Cagliari, 09042 Monserrato (Cagliari), Italy, ^cUniversity of California Irvine, Irvine, CA 92697, USA, ^dInstitute of Physics, Academy of Sciences of the Czech Republic, 182 21, Czech Republic, ^eCERN, CH-1211 Geneva, Switzerland, ^fCornell Uni-

- 2013-034 (2013).
- [9] G. Aad *et al.* (ATLAS Collaboration), Phys. Rev. D **91**, 012006 (2015).
- [10] S. Chatrchyan *et al.* (CMS Collaboration), Phys. Rev. D **89**, 092007 (2014).
- [11] S. Chatrchyan *et al.* (CMS Collaboration), Eur. Phys. J. C **74** (2014) 3076.
- [12] G. Aad *et al.* (ATLAS Collaboration), ATLAS-CONF-2013-040 (2013).
- [13] G. Aad *et al.* (ATLAS Collaboration), Phys. Lett. B **726**, 120 (2013).
- [14] S. Chatrchyan *et al.* (CMS Collaboration), Phys. Rev. Lett. **110**, 081803 (2013).
- [15] S. Chatrchyan *et al.* (CMS Collaboration), J. High Energy Phys. 01 (2014) 096.
- [16] V. Khachatryan *et al.* (CMS Collaboration), arXiv:1411.3441 [hep-ex].
- [17] T. Aaltonen *et al.* (CDF and D0 Collaborations), Phys. Rev. Lett. **109**, 071804 (2012).
- [18] T. Aaltonen *et al.* (CDF and D0 Collaborations), Phys. Rev. D **88**, 052014 (2013).
- [19] T. Aaltonen *et al.* (CDF Collaboration), Phys. Rev. D **88**, 052013 (2013).
- [20] V. M. Abazov *et al.* (D0 Collaboration), Phys. Rev. D **88**, 5, 052011 (2013).
- [21] CDF Collaboration, “Constraints on Models for the Higgs Boson with Exotic Spin and Parity with CDF”, Submitted to Phys. Rev. Lett., FERMILAB-PUB-15-012-E (2015), [arXiv:1501.04875].
- [22] V. M. Abazov *et al.* (D0 Collaboration), Phys. Rev. Lett. **113**, 161802 (2014).
- [23] J. Ellis, D. S. Hwang, V. Sanz, and T. You, J. High Energy Phys. 11 (2012) 134.
- [24] D. J. Miller, S. Y. Choi, B. Eberle, M. M. Mühlleitner, and P. M. Zerwas, Phys. Lett. B **505**, 149 (2001).
- [25] S. Chatrchyan *et al.* (CMS Collaboration), Nature Physics **10**, 557 (2014).
- [26] S. Chatrchyan *et al.* (CMS Collaboration), J. High Energy Phys. 05 (2014) 104.
- [27] G. Aad *et al.* (ATLAS Collaboration), J. High Energy Phys. 09 (2012) 070.
- [28] G. Aad *et al.* (ATLAS Collaboration), Submitted to J. High Energy Phys., CERN-PH-EP-2014-262 (2014), [arXiv:1501.04943].
- [29] S. Chatrchyan *et al.* (CMS Collaboration), Phys. Rev. D **89**, 012003 (2014).
- [30] G. Aad *et al.* (ATLAS Collaboration), J. High Energy Phys. 01 (2015) 069.
- [31] T. Aaltonen *et al.* (CDF Collaboration), Phys. Rev. Lett. **109**, 111804 (2012).
- [32] V. M. Abazov *et al.* (D0 Collaboration), Phys. Rev. D **88**, 052008 (2013).
- [33] T. Aaltonen *et al.* (CDF Collaboration), Phys. Rev. Lett. **109**, 111803 (2012).
- [34] V. M. Abazov *et al.* (D0 Collaboration), Phys. Rev. D **88**, 052010 (2013).
- [35] T. Aaltonen *et al.* (CDF Collaboration), Phys. Rev. D **87**, 052008 (2013).
- [36] V. M. Abazov *et al.* (D0 Collaboration), Phys. Lett. B **716**, 285 (2012).
- [37] Positions and angles are expressed in a cylindrical coordinate system, with the z axis directed along the proton beam. The polar angle θ is defined with respect to the proton beam direction. The missing transverse en-
- ergy is defined as a sum over calorimeter towers, $\vec{E}_T = -\sum_i E_i \sin \theta_i \hat{n}_i$, where i is the calorimeter tower number, and \hat{n}_i is a unit vector perpendicular to the beam axis and pointing to the i th tower. The reconstructed \vec{E}_T is corrected for contributions from muons which register less energy in the calorimeter, and for jet energy corrections. The scalar magnitude of \vec{E}_T is denoted E_T .
- [38] D. Acosta, *et al.* (CDF Collaboration), Phys. Rev. D **71**, 032001 (2005); A. Abulencia, *et al.* (CDF Collaboration), J. Phys. G **34**, 2457 (2007).
- [39] V. M. Abazov *et al.* (D0 Collaboration), Nucl. Instrum. Methods A **565**, 463 (2006); M. Abolins *et al.*, Nucl. Instrum. Methods A **584**, 75 (2008); R. Angstadt *et al.*, Nucl. Instrum. Methods A **622**, 298 (2010).
- [40] T. Sjöstrand, S. Mrenna, and P. Skands, J. High Energy Phys. 05 (2006) 026. We use PYTHIA version 6.216 to generate the Higgs boson signal events.
- [41] H. L. Lai, J. Huston, S. Kuhlmann, F. I. Olness, J. F. Owens, D. E. Soper, W. K. Tung, and H. Weerts, Phys. Rev. D **55**, 1280 (1997).
- [42] J. Alwall, M. Herquet, F. Maltoni, O. Mattelaer, and T. Stelzer, J. High Energy Phys. 06 (2011) 128.
- [43] J. Baglio and A. Djouadi, J. High Energy Phys. 10 (2010) 064.
- [44] G. Ferrera, M. Grazzini, and F. Tramontano, Phys. Rev. Lett. **107**, 152003 (2011).
- [45] O. Brein, A. Djouadi, and R. Harlander, Phys. Lett. B **579**, 149 (2004).
- [46] M. L. Ciccolini, S. Dittmaier, and M. Kramer, Phys. Rev. D **68**, 073003 (2003).
- [47] LHC Higgs Cross Section Working Group, arXiv:1201.3084.
- [48] A. Djouadi, J. Kalinowski, and M. Spira, Comput. Phys. Commun. **108**, 56 (1998).
- [49] A. Bredenstein, A. Denner, S. Dittmaier, and M. M. Weber, Phys. Rev. D **74**, 013004 (2006) and J. High Energy Phys. 02 (2007) 080;
A. Bredenstein, A. Denner, S. Dittmaier, A. Mück, and M. M. Weber, <http://omnibus.uni-freiburg.de/~sd565/programs/prophecy4f/> (2010).
- [50] J. M. Campbell and R. K. Ellis, Phys. Rev. D **60**, 113006 (1999).
- [51] U. Langenfeld, S. Moch, and P. Uwer, Phys. Rev. D **80**, 054009 (2009).
- [52] T. Aaltonen *et al.* (CDF and D0 Collaborations), Phys. Rev. D **86**, 092003 (2012).
- [53] A. D. Martin, W. J. Stirling, R. S. Thorne, and G. Watt, Eur. Phys. J. C **63**, 189 (2009).
- [54] N. Kidonakis, Phys. Rev. D **74**, 114012 (2006).
- [55] In the CDF analyses, backgrounds from SM processes with electroweak gauge bosons or top quarks are modeled using PYTHIA [40], ALPGEN [56], MC@NLO [57], and HERWIG [58]. For D0, these backgrounds are modeled using PYTHIA, ALPGEN, and SINGLETOP [59], with PYTHIA providing parton showering and hadronization for all the generators.
- [56] M. L. Mangano, M. Moretti, F. Piccinini, R. Pittau, and A. D. Polosa, J. High Energy Phys. 07 (2003) 001.
- [57] S. Frixione and B.R. Webber, J. High Energy Phys. 06 (2002) 029.
- [58] G. Corcella, I. G. Knowles, G. Marchesini, S. Moretti, K. Odagiri, P. Richardson, M. H. Seymour, and

- B. R .Webber, J. High Energy Phys. 01 (2001) 010.
- [59] E. E. Boos, V. E. Bunichev, L. V. Dudko, V. I. Savrin, and V. V. Sherstnev, Phys. Atom. Nucl. 69, 1317 (2006).
- [60] A heavy-flavor jet is a reconstructed cluster of calorimeter energies associated with particles produced in the hadronization and decay of a b or c quark.
- [61] A b -tagged jet is a jet identified as being consistent with that expected from the decay products of a b quark based on properties such as the presence of displaced track vertices or soft leptons.
- [62] T. Aaltonen *et al.* (CDF Collaboration), Phys. Rev. Lett. **109**, 111802 (2012).
- [63] V. M. Abazov *et al.* (D0 Collaboration), Phys. Rev. Lett. **109**, 121802 (2012).
- [64] J. Freeman, T. Junk, M. Kirby, Y. Oksuzian, T. J. Phillips, F. D. Snider, M. Trovato, and J. Vizan *et al.*, Nucl. Instrum. Methods A **697**, 64 (2013).
- [65] V. M. Abazov *et al.* (D0 Collaboration), Nucl. Instrum. Methods A **620**, 490 (2010).
- [66] V. M. Abazov *et al.*, (D0 Collaboration), Nucl. Instrum. Methods A **763**, 290 (2014).
- [67] T. Aaltonen *et al.* (CDF Collaboration), Phys. Rev. Lett. **105**, 251802 (2010).
- [68] L. Breiman, Machine Learning **45**, 5 (2001).
- [69] A. Hocker *et al.*, Proc. Sci., ACAT2007 (2007) 040 [arXiv:physics/0703039].
- [70] S. Klimenko, J. Konigsberg, and T. M. Liss, FERMILAB-FN-0741 (2003).
- [71] T. Junk, Nucl. Instrum. Methods A **434**, 435 (1999); A. L. Read, J. Phys. G **28**, 2693 (2002).
- [72] W. Fisher, FERMILAB-TM-2386-E (2006).
- [73] See Supplemental Material at <http://link.aps.org/> supplemental/xx.xxxx/PhysRevLett.xxx.xxxxxx for additional figures.
- [74] ATLAS and CMS Collaborations, ATLAS-PHYS-PUB-2011-011, CMS NOTE-2011/005 (2011).

Supplemental Material

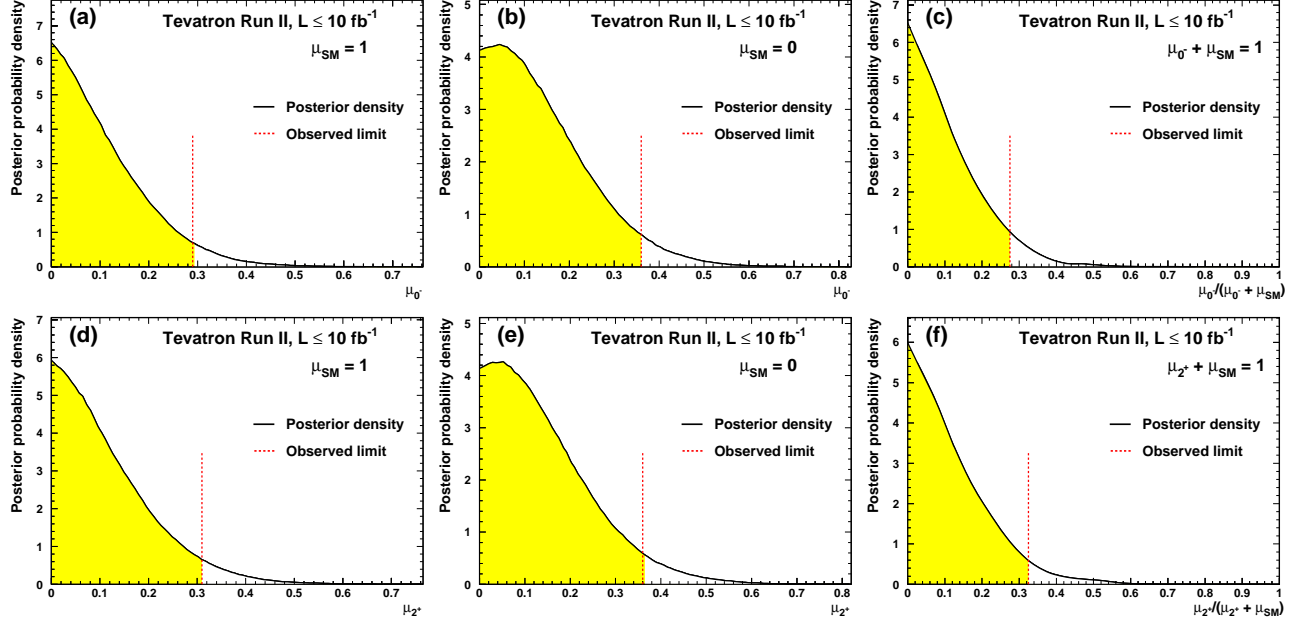


FIG. 4: Posterior probability density distributions for the combined searches for exotic $J^P = 0^-$ and $J^P = 2^+$ bosons. (a) The posterior probability density as a function of μ_{0^-} assuming $\mu_{SM} = 1$ and a uniform prior density for non-negative μ_{0^-} , (b) the posterior probability density as a function of μ_{0^-} assuming $\mu_{SM} = 0$ and a uniform density for non-negative μ_{0^-} , and (c) the posterior probability density as a function of the fraction of exotic boson production, $\mu_{0^-}/(\mu_{0^-} + \mu_{SM})$, assuming $\mu_{0^-} + \mu_{SM} = 1$, and a uniform prior density for non-negative values of the fraction. The dashed vertical lines indicate the observed limits. Figures (d), (e), and (f) show the corresponding results for the $J^P = 2^+$ boson searches.

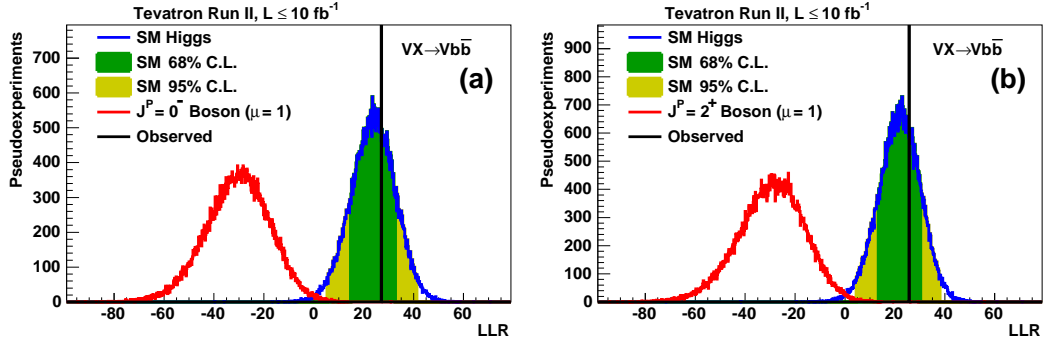


FIG. 5: Distributions of LLR for the combined CDF and D0 searches for (a) the pseudoscalar ($J^P = 0^-$) boson, and (b) the graviton-like ($J^P = 2^+$) boson. The LLR distributions are shown separately assuming that an exotic particle is present with $\mu_{exotic} = 1$ plus SM backgrounds, and if the SM Higgs boson plus SM backgrounds are present. The observed values of LLR are shown with vertical lines. Shaded regions show the 68% and 95% confidence level regions on the distributions assuming the SM Higgs boson is present, centered on the median expectation.